Pergamon

Cement and Concrete Research 32 (2002) 87–90

CEMENT AND CONCRETE RESEARCH

Investigation of characterizing methods for the microstructure of cement

Erich Robens[a,*], Bernhard Benzler[b], Gunter Büchel[a,1], Horst Reichert[c], Kai Schumacher[a,2]

[a]*Institut für Anorganische Chemie und Analytische Chemie der Johannes Gutenberg-Universität, Duesbergweg 10-14, D-55099 Mainz, Germany*
[b]*Mettler Toledo GmbH, Ockerweg 3, D-35379 Giessen, Germany*
[c]*POROTEC GmbH, Niederhofheimer Straße 55a, D-65719 Hofheim/Ts., Germany*

Received 25 September 1999; accepted 24 July 2001

Abstract

Volumetric, gravimetric, calorimetric, flow methods, mercury porosimetry and laser granulometry were used to investigate the surface structure and the sorption behavior of industrial cements and hydrated cement paste. The suitability of the measuring methods is assessed.

Keywords: Hydration; Microstructure; Surface; Adsorption; Cement paste

1. Introduction

To control the production of cement and to predetermine the features of concrete, it is necessary to know the microstructure of cement as characterized by the grain size distribution and the specific surface area. For concrete and cement stone, characterizing parameters are the specific surface area and the pore size distribution [1]. Commonly, the specific surface area is measured by means of flow methods with air, mostly Blaine test and by nitrogen sorption at 77 K. Today, methods of particle size measurement are preferred in which the particles are conveyed individually by gas or liquid flow through a slit. There, the particles are counted and the diameter determined optically or by electrical sensing, respectively. The pore size distribution is derived from the nitrogen isotherm (meso- and micropores) and from mercury intrusion measurements (meso- and macropores). Through the water sorption isotherm, it is possible to observe the reaction of the sample material with water. Recently, thermoporometry was applied to determine the pore size distribution in the mesopore range as a function of the hardening process of cement stone [2,3]. The present paper deals with the comparison of different measurement methods in order to evaluate their suitability for the microstructure analysis of cement and hardened cement paste.

2. Materials and instrumentation

We investigated samples of typical cements (Tables 1 and 2) supplied from Dyckerhoff, and we compared them with results published by Willems [4] using samples of

Table 1
Cement characteristics

Product	Type	Manufacturer	Density (g cm^{-3})	Volume median diameter (μm)
White	Portland	Dyckerhoff	3.10	13.6
PZ double	Portland	Dyckerhoff	3.10	11.4
PZ triple	Portland	Dyckerhoff	3.10	7.9
EPZ normal	Iron Portland	Dyckerhoff	3.04	15.8
Aquadur	Blast furnace	Dyckerhoff	3.00	12.1
PC	Portland	ENCI	3.13	13.0
PBC	Blast furnace	CEMIJ	2.97	11.3

* Corresponding author. Schlesierstr. 5, D-61381 Friedrichsdorf, Germany. Tel.: +49-6172-778584; fax: +49-6172-777070.
E-mail address: erich.robens@t-online.de (E. Robens).
[1] Present address: ALCOA AG, Lyoner Str. 30, D-60528 Frankfurt am Main, Germany.
[2] Present address: Degussa AG, AS-FA-AE/F, Rodenbacher Chaussee 4, D-63457 Hanau, Germany.

0008-8846/02/$ – see front matter
PII: S0008-8846(01)00633-0

Table 2
Addresses of the manufacturers

Cahn Instrument, 5225 Verona Road, Bldg. 1, Madison, WI 53711-4495, USA
THERMO Finnigan, ThermoQuest Italia S.P.A., Str. Rivoltana, I-20090 Rodano, Milano, Italy
CEMIJ-ENCI Maastricht, Postbus 1, NL-6200 AA Maastricht, The Netherlands
Dyckerhoff, Biebricher Straße 69, D-65203 Wiesbaden, Germany
ENCI Ymmiden, Postbus 4262, NL-1970 AL Ymmiden, The Netherlands
Mettler-Toledo, CH-8606 Greifensee, Switzerland
Quantachrome, 5 Aerial Way, Syosset, NY 11791-9011, USA
Sympatec, Burgstädter Straße 6, D-38678 Clausthal-Zellerfeld, Germany
WASAGCHEMIE Sythen, Werkstraße 111, D-45721 Haltern, Germany
Surface Measurement Systems, 3 Warple Mews, Warple Way, London, W3 ORF, UK

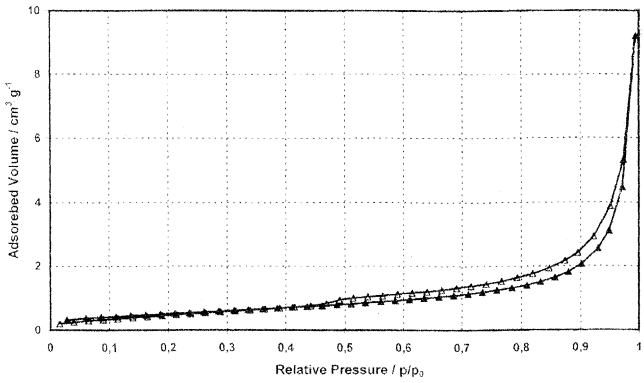

Fig. 1. Nitrogen sorption isotherm at 77 K on hydrated Portland cement Dyckerhoff white.

ENCI and CEMIJ. Measurements were performed with the original cement powder and with samples mixed with a surplus of water and subsequently dried in air at 22–25 °C and 30% relative humidity for 24 h. The resulting cement stone can be easily crushed to give a powder. Hydrated cement paste is a heterogeneous material consisting of many different hydrated products. In its dried state, it exhibits a layered gel structure with water between the layers [5].

The grain size distribution of cement powder was determined with a laser granulometer (Sympatec HELOS VECTRA) and the specific surface area with a WASAG automatic Blaine test apparatus. Nitrogen sorption isotherms at 77 K were measured with a volumetric apparatus (Quantachrome AUTOSORB 6 B). From the isotherm and by means of mercury porosimetry (THERMO Finnigan PASCAL 140/440), pore size distributions were calculated. All measurements fitted the standard rules of ISO, ASTM or DIN [6].

Water sorption isotherms were measured gravimetrically with a stepwise varied relative humidity (Surface Measurement Systems DVS1). The sample placed in the pan of a symmetric Cahn balance is exposed to a continuous flow of air of controlled humidity, to achieve quickly equilibrium. Thermoporometry [7,8] was performed using a differential scanning calorimeter (Mettler-Toledo DSC 821).

3. Results and discussion

The results of surface area and pore volume determination are summarized in Table 3. S_{grain} denotes the surface area calculated from laser granulometry; S_{Blaine} from the Blaine test [9]. The different measuring principles cause systematic differences in the results: S_{grain} was always found to be larger by a factor of 1.3. Prior to the measurement of the nitrogen isotherm, the samples were degassed for 12 h in high vacuum (2×10^{-2} Pa) at a temperature of 150 °C. S_{BET} and S_{BJH} were calculated from the nitrogen isotherm using the two-parameter equation of Brunauer et al. [10] and the method of Barrett et al. [11], respectively. The latter was applied to both the adsorption and desorption branch of the isotherm. The larger surface which was always detected by the sorption methods included the inner surface of the open pores, whereas S_{Blaine} and S_{grain} reflects only the outer particle surface. The nitrogen isotherms of all samples

Table 3
Specific surface area and pore volume from the nitrogen isotherm of cement and (^{h}) hydrated and dried cement paste

Sample	S_{grain} ($m^2\ g^{-1}$)	S_{Blaine} ($m^2\ g^{-1}$)	S_{BET} ($m^2\ g^{-1}$)	S_{BJH} (ads. $m^2\ g^{-1}$)	S_{BJH} (des. $m^2\ g^{-1}$)	S_{H20} ($m^2\ g^{-1}$)	V_{BJH} (ads. $mm^3\ g^{-1}$)	V_{BJH} (des. $mm^3\ g^{-1}$)	V_G ($mm^3\ g^{-1}$)	V_{DR} ($mm^3\ g^{-1}$)
White	0.47	0.36	1.42	1.80	2.32		9.02	9.22	8.88	0.59
White^h			3.55	4.13	5.36	5.8	26.54	27.17	26.33	1.46
PZ double	0.48	0.36	1.07	1.22	1.82		7.00	7.49	6.81	0.47
PZ double^h			1.09	1.59	2.63		8.58	8.92	8.54	0.46
PZ triple	0.67	0.53	1.54	1.85	3.17		12.93	13.38	12.81	0.64
PZ triple^h			3.80	4.02	5.27		27.89	28.43	27.85	1.59
EPZ normal	0.39	0.30	0.37	0.48	0.84		2.94	3.06	2.90	0.15
EPZ normal^h			2.76	2.96	4.34	8.4	22.00	22.79	21.97	1.21
Aquadur	0.45	0.36	1.22	1.58	2.47		7.40	7.92	7.27	0.52
Aquadur^h			2.20	2.56	3.41		13.23	13.50	13.11	0.92
PC		0.42	1.71	1.90	3.02	10.9	13.02	13.92	13.01	0.98
PBC		0.30	1.05	1.31	2.03	11.6	6.23	6.80	6.70	0.49

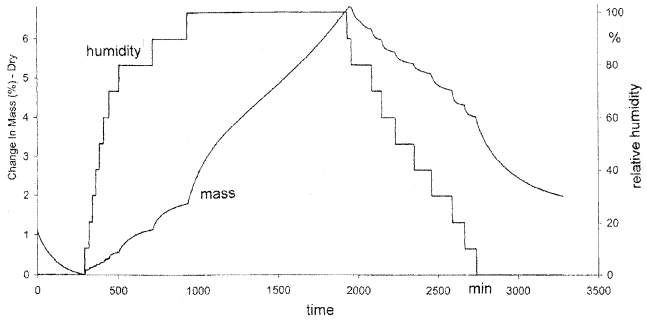

Fig. 2. Stepwise measurement of water adsorption and desorption at 25 °C on hydrated Dyckerhoff white.

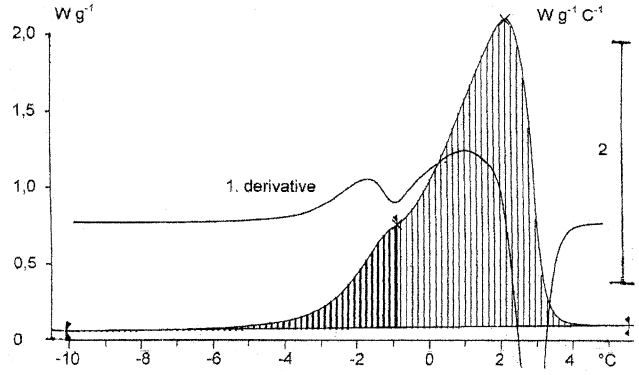

Fig. 4. Thermoporometric curve on hydrated Portland cement double.

correspond to type II isotherm of the IUPAC classification [12], Fig. 1 demonstrates an example. The small hysteresis loop of the isotherm is due to the sum of mesopores within the particles and interparticulate voids. From the isotherms, the cumulative mesopore volume V_{BJH} and the Gurwitsch-volume V_G [13] were calculated. The pore size distributions reveal a mesopore structure with diameters in the range 1–2 nm. A part of the total pore volume was due to micropores V_{DR}, derived by the method of Dubinin and Radushkevich [14]. After hydration of the cement, the specific surface area and the pore volume increased as a result of the layer structure developed. The pore size distribution obtained by mercury porosimetry exhibited a broad pore spectrum in the range 0.1–50 μm for all samples which is attributed to interparticulate voids.

The water vapor adsorption proceeds slowly so that equilibrium could not be established within a reasonable time (Fig. 2). Due to the swelling process, all isotherms exhibit a very large hysteresis loop, going down to zero relative pressure (Fig. 3).

This may be explained as follows: The dried hydrated cement paste has a layered gel structure with interlayers of water. At low relative water vapor pressure first, the outer surface of the gel and the walls of the free pores are wetted. Near saturation pressure the water is able to penetrate into the layered gel structure, which is demonstrated by the steep increase of the isotherm at about 90% relative humidity. Upon decreasing water vapor pressure first, the multilayers at the outer surface are reduced, the free pores are emptied successively and, finally, at very low relative pressure, the water between the layers dries out, leaving behind the initial gel structure with interlayer water. Willems [4] proved that, at each stage, an equilibrium can be adjusted. The time needed, however, can cover days and weeks. The values of the specific surface area S_{H2O} in Table 3 are calculated by means of the two-parameter BET equation. Our values are less correct, because equilibrium was not reached. The pore size distributions indicate frequent pore diameters below 2 nm.

For most samples, only one broad peak corresponding to the freezing of bulk water was observed by thermoporometry. This peak is distorted towards higher temperature because melting of the big water mass surrounding the sample is time consuming, and the x-axis indeed is a time-axis. An example in which a second peak could be detected is shown in Fig. 4. This peak is near the upper detection limit of -1 °C, corresponding to a pore width >100 nm. Since that peak is overlapped for the most part by the bulk water peak, the calculation of a pore volume and a pore size distribution seems to be unsuitable.

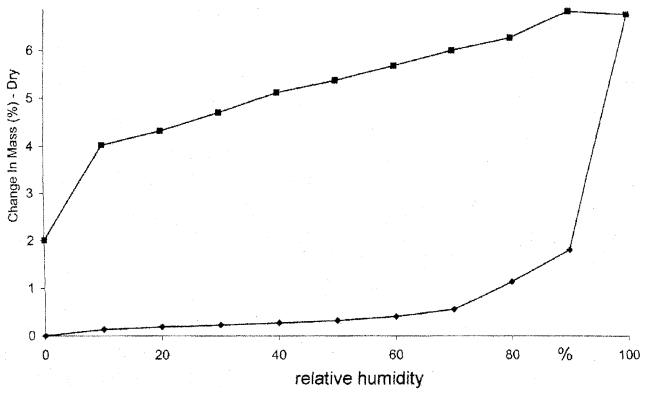

Fig. 3. Water sorption isotherm at 25 °C on hydrated Dyckerhoff white.

4. Conclusions

The specific surface area is a central value to characterize the microstructure of cement and hardened cement paste, and in principle all the discussed methods are allowing for its determination. It is, however, an integral value and much more information can be obtained from both the particle size distribution and from the pore size distribution.

The values of specific surface area recorded in Table 3 depend strongly on the measuring method. Values from the Blaine-test describe the outer surface of the cement grains. Apart from a systematic deviation due to the different measuring principles, they give the same information as those derived from the grain size distribution.

For processing cement powder with water, the surface area and the pore volume accessible for water are relevant parameters. Commonly, the parameters are calculated from the nitrogen isotherm at 77 K. Also, cement paste may be characterized in this way. Unfortunately, prior to the measurement, it is necessary to outgas the sample in vacuum at elevated temperature. Hereby, the stronger bound water between the layers of the gel is removed and additional pores may be opened up. Also, cooling down to the measurement temperature of 77 K may affect the porous structure. The isotherms are evaluated in various ways on the basis of different models (BET, BJH and Gurwitsch). As can be seen in Table 3, the results differ systematically. On account of the lack of quantitative theories, the measurements should be performed according to the standardization rules so that the results can be used as comparative figures. It should be kept in mind that the water molecule is smaller than nitrogen, and thus the accessible surface and pore volume indeed are larger.

Water sorption isotherms allow for the observation of hydration, development of the gel structure and its drying. Since the measurements are time consuming and equilibrium values are uncertain, extrapolation by analysis of the kinetic curves should be applied [15]. When curtailing the measuring time by such an extrapolation method the adsorption branch of the water isotherm could well be used to determine the specific surface area and the pore size distribution [16]. This would be very favorable, because in this way just the surface and pores accessible for the reactant water could be determined. A source of error is swelling processes with water.

Mercury porosimetry is widely used in the investigation of cement products [17–19]. We found pores in the high meso- and the macropore range, which we attribute to interparticulate voids. To detect pores below 2 nm, much higher pressures are required and that is beyond the range of commercial instruments.

In the present measurements, the restricted range of thermoporometry became obvious. In accordance with the results of mercury porosimetry with thermoporometry, we found pores above 0.1 μm, which is the upper practical limit of the method. Pores with diameter below 2 nm are revealed from the nitrogen and the water sorption isotherms; this is below the lower detection limit of thermoporometry. Thermoporometry may be useful for characterizing concrete and possibly cement stone after an extended hardening process [20]. Recent reports [2,3] are not detailed enough to judge this and additional investigations are necessary.

Acknowledgments

We are indebted to Mr. T. Volk, Dyckerhoff for supplying us with samples and their characteristic features.

References

[1] R.Sh. Mikhail, E. Robens, Microstructure and Thermal Analysis of Solid Surfaces, Wiley, Chichester, 1983.
[2] T. Chaussadent, G. Platret, R. Lavarenne, A. Raoof, J.-P. Guilbaud, Sorption of water vapor and thermoporometry. Investigation of the texture of "ideal" porous materials and possible applications to concrete, Bull. Lab. Ponts Chaussees 208 (1997) 67–74.
[3] A.V. Usherov-Marshak, V.P. Sopov, V.I. Kondraschenko, The regularities of forming and modeling the microstructure at the early stages of cement stone hardening, in: H. Justnes (Ed.), Proc. 10th Int. Congr. Chem. Cem. vol. 2, Amarkai, Goeteborg, 1997.
[4] H.H. Willems, Creep behaviour and microstructure of hardened cement pastes, Thesis, T.U. Eindhoven, 1985.
[5] K.G. Krasilnikov, N.N. Skoblinskaya, The change of cement stone porous structure in the process of expansion and shrinkage at adsorption of water, Proc. Int. Symp. RILEM/IUPAC on the Pore Structure and Properties or Materials, Part 4, Praha, 1973.
[6] E. Robens, K.-F. Krebs, K. Meyer, K.K. Unger, Standardization of sorption measurements and reference materials for dispersed and porous solids, in: A. Dabrowski (Ed.), Adsorption and its Application in Industry and Environmental Protection, Vol. 1. Studies in Surface Science and Catalysis, vol. 120 A, Elsevier, Amsterdam, 1999, pp. 95–116.
[7] J.-F. Quinson, M. Astier, M. Brun, Determination of surface areas by thermoporometry, Appl. Catal. 30 (1987) 125–130.
[8] J.-F. Quinson, M. Brun, Progress in thermoporometry, in: K.K. Unger, J. Rouquerol, K.S.W. Sing, H. Kral (Eds.), Characterization of Porous Solids, Elsevier, Amsterdam, 1988, pp. 307–315.
[9] R.L. Blaine, Standard for the determination of the fineness of Portland cement by air flow, Blaine method, ASTM C 204 (1968), ASTM Bull. No. 12 B. Ditto: Federal Test Method Standard 158 + Method 2101, AASHTO T 153.
[10] S. Brunauer, P.H. Emmett, E. Teller, Adsorption of gases in multimolecular layers, J. Am. Chem. Soc. 60 (1938) 309.
[11] E.P. Barrett, L.G. Joyner, P.P. Halenda, The determination of pore volume and area distribution in porous substances: I. Computation from nitrogen isotherms, J. Am. Chem. Soc. 73 (1951) 373–380.
[12] F. Rouquerol, J. Rouquerol, K. Sing, Adsorption by Powders and Porous Solids, Academic Press, San Diego, 1999, pp. 439–442.
[13] L. Gurwitsch, J. Phys. Chem. Soc. Russia 47 (1915) 805 (See D.N. Broad, A.G. Foster, The sorption of condensable vapours by porous solids: Part II. The validity of Gurwitsch's rule, J. Chem. Soc. (1945) 366–371.).
[14] M.M. Dubinin, The potential theory of adsorption of gases and vapours for adsorbents with energetically nonuniform surface, Chem. Rev. 60 (1969) 235.
[15] E. Robens, J.A. Poulis, C.H. Massen, Fast gas adsorption measurements for complicated adsorption mechanisms, in: V.A. Tertykh (Ed.), Proceedings of the 28th International Conference on Vacuum Microbalance Techniques, 1999, Kyiv. Journal of Thermal Analysis and Calorimetry 62, (2000) 429–433.
[16] A.J. Juhola, Manufacture, pore structure and application of activated carbons, Kemia-Kemi 4 (1977) 11, 543–551+12, 653–661.
[17] H.L. Ritter, L.C. Drake, Pore size distribution in porous materials: I. Pressure porosimeter and determination of complete macropore size distributions, Ind. Eng. Chem. Anal. Ed. 17 (1945) 782–786.
[18] H.L. Ritter, L.C. Drake, Pore size distribution in porous materials: II. Macropore size distributions in some typical porous substances, Ind. Eng. Chem. Anal. Ed. 17 (1945) 787–791.
[19] H.M. Rootare, C.F. Prenzlow, Surface areas from mercury porosimeter measurements, J. Phys. Chem. 71 (8) (1967) 2733–2736.
[20] N. Stockhausen, H. Dorner, B. Zech, J. Setzer, Untersuchung von Gefriervorgängen in Zementstein mit Hilfe der DTA, Cem. Concr. Res. 9 (1979) 783–794.